June, 1992] Bull. Chem. Soc. Jpn., 65, 1585—1590 (1992)

X-Ray Structure, Ligand Substitution, and Other Properties of Trinuclear Ruthenium Complex, $[Ru_3(\mu_3\text{-}O)(\mu\text{-}C_6H_5COO)_6(py)_3](PF_6)$ (py=pyridine), and X-Ray Structure of Dinuclear Ruthenium Complex, $[Ru_2(\mu\text{-}C_6H_5COO)_4Cl]$

Masaaki Abe, Yoichi Sasaki,*,† Tadashi Yamaguchi,
and Tasuku Ito*
Department of Chemistry, Faculty of Science, Tohoku University, Aoba-ku, Sendai 980
(Received January 21, 1992)

Crystal structure of an oxo-benzoate-bridged trinuclear ruthenium complex, $[Ru_3(\mu_3\text{-}O)(\mu\text{-}C_6H_5COO)_6(py)_3](PF_6)$ (py = pyridine) (**1**), was determined for the first time for the complexes with a Ru3(III,III,III)(μ_3-O) core. The complex crystallizes in hexagonal space group $P6_3$ with a=13.619(6), c=19.204(9) Å, V=3085(3) Å^3, and Z=2. The Ru···Ru distance of 3.350(2) Å is similar to those of the trinuclear complexes of other metal ions, $[M^{III}{}_3(\mu_3\text{-}O)(\mu\text{-}RCOO)_6(L)_3]^+$ (L = neutral unidentate ligand). The complex in 0.1 M $(n\text{-}C_4H_9)_4NPF_6$-acetonitrile at 20 °C shows four reversible one-electron processes at $E_{1/2}$=+1.58, +0.71, −0.26, and −1.54 V vs. Ag/Ag$^+$ (0.1 M $AgClO_4$). It undergoes pyridine-d_5 exchange with the first-order rate constant, 4.9×10^{-6} s^{-1} at 60 °C ([**1**] = 4.7 mM, [py-d_5] = 387 mM). Small modification of the synthetic procedure of the trinuclear complex leads to the precipitation of the crystals of well-known type of dimeric ruthenium (II,III) complex, $[Ru_2(\mu\text{-}C_6H_5COO)_4Cl]$, which crystallizes in monoclinic space group $C2/c$ with a=21.668(10), b=10.741(8), c=12.797(5) Å, β=110.22(4)°, V=2795(3) Å^3, and Z=4. The crystal contains infinite zig-zag chain of ···Cl–Ru–Ru–Cl···along c-axis with Ru–Ru–Cl of 175.5(1)°, Ru–Cl–Ru of 118.1(1)°, and the Ru–Ru distance of 2.290(1) Å.

Oxo-centered carboxylate-bridged trinuclear complexes, $[M_3(\mu_3\text{-}O)(\mu\text{-}RCOO)_6(L)_3]^+$ (L = unidentate neutral ligand) are known for wide range of trivalent transition metal ions.[1] Ruthenium complexes[2] are of particular interest with their variegated redox behavior, strong metal–oxo–metal interactions manifested by intense visible absorption[3–7] and magnetic behavior.[8] However, relatively few works have been carried out for the complexes with carboxylate ligands other than acetate.[3–9] Also, there has been no structural determination reported for the Ru_3 complexes although structures for all other metals were determined.[1] Only report for the triruthenium complex is for the one-electron reduced species, $[Ru_3{}^{II,III,III}(\mu_3\text{-}O)(\mu\text{-}CH_3COO)_6(PPh_3)_3]$ (PPh_3 = triphenylphosphine).[9]

We have studied benzoate derivatives of μ_3-oxo-triruthenium complex for the comparison with the acetate derivatives. Neutral complex, $[Ru_3(\mu_3\text{-}O)(\mu\text{-}C_6H_5COO)_6(H_2O)_3]$, in which Ru_3 are in the formal oxidation state (II,III,III), was previously reported,[3] although neither synthetic procedure nor structural evidence has been shown. $[Ru_3(\mu_3\text{-}O)(\mu\text{-}C_6H_5COO)_6(py)_3](PF_6)$ (**1**) is its new derivative with pyridine ligands at the terminal positions and with the Ru_3 oxidation state of (III,III,III). Synthesis and X-ray structure of **1** are described along with some chemical properties. Terminal ligand substitution reaction has also been studied briefly.

During the study, we have isolated crystals of $[Ru_2(\mu\text{-}C_6H_5COO)_4Cl]$ (**2**), which consists of known structural type of tetracarboxylate-bridged dimer.[10] Crystal structure of **2** is also reported in this paper. The isolation of dimeric complex seems to have significance in view of the synthetic route of the carboxylate-bridged complexes.

Experimental

Materials. Acetonitrile used in electrochemical measurements was distilled twice over P_2O_5 and once over CaH_2. Other reagents were used as received.

Syntheses. $[Ru_3(\mu_3\text{-}O)(\mu\text{-}C_6H_5COO)_6(py)_3](PF_6)$ (1). To a hot suspension of benzoic acid (47 g, 385 mmol) and NaOH (1.6 g, 40 mmol) in C_2H_5OH (150 cm^3), $RuCl_3\cdot nH_2O$ (1.0 g) was added. The mixture was refluxed for ca. 1 h to give a blue-green solution.[18] After evaporation to dryness, CH_3OH (100 cm^3) and pyridine (1 cm^3) were added to the residue, and the resulting solution was further refluxed for 1 h. After addition of NH_4PF_6 (0.5 g, 3.1 mmol), the solution was left overnight in a refrigerator to give dark blue powder of **1**. Single crystals of **1** suitable for X-ray analysis were obtained from slow recrystallization (ca. a month) from CH_3CN/CH_3OH (1 : 2 (v/v)) at 0 °C.

Anal. Found: C, 48.02; H, 2.99; N, 3.02%. Calcd for $C_{57}F_6H_{45}N_3O_{13}PRu_3$: C, 47.93; H, 3.18; N, 2.94%; ^{1}H NMR[19] (CD_3CN) δ=1.11 (6H, s, py-2,6-H), 6.06 (6H, t, py-3,5-H), 6.53 (3H, t, py-4-H), 7.68 (12H, t, Ph-3,5-H), 7.89 (6H, t, Ph-4-H), 9.41 (12H, d, Ph-2,6-H); ^{13}C NMR (CD_3CN) δ=104.50 (py-2,6-C), 115.22 (Ph-1-C), 129.53 (py-4-C), 130.05 (Ph-2,6 or 3,5-C), 131.08 (Ph-3,5 or 2,6-C), 134.94 (Ph-4-C), 138.86 (py-3,5-C), 183.06 (C=O); FAB MS (NBA as a matrix) m/z 1284 ([M]$^+$),[20] 1205 ([M-py]$^+$), 1127 ([M-2py]$^+$), 1047 ([M-3py]$^+$), 1005 ([M-2py-$C_6H_5COO^-$]$^+$), 926 ([M-3py-$C_6H_5COO^-$]$^+$); IR (KBr) 3060, 1600, 1530, 1495, 1485, 1450, 1400, 1218, 1178, 1070, 1022, 840, 758, 710, 695, 690, 558, 515, 505 cm^{-1}.

$[Ru_2(\mu\text{-}C_6H_5COO)_4Cl]$ (2). A mixture of benzoic acid (7.8 g, 64 mmol), NaOH (0.1 g, 2.5 mmol), and $RuCl_3\cdot nH_2O$ (1.0 g) in C_2H_5OH (150 cm^3) was refluxed for 4 h and filtered. Resulted blue-green solution was allowed to stand for ca. two weeks at room temperature, yielding red-brown crystals (150 mg). Anal. Found: C, 46.44; H, 2.84; Cl, 5.41%. Calcd for $C_{28}ClH_{20}O_8Ru_2$: C, 46.57; H, 2.80; Cl, 4.91%. IR data

---

† Present address: Department of Chemistry, Faculty of Science, Hokkaido University, Kita-ku, Sapporo 060.

were consistent with the reported result.[11]

X-Ray Structure Determination. For compounds **1** and **2**, data collection experiments and structure analyses were carried out in the same way. A Rigaku AFC-5R four circle diffractometer with Mo *Kα* (λ=0.71069 Å) radiation was used. Lorentz and polarization factors were corrected. The absorption correction was made by the numerical method on Gaussian integration for **1**, and by the empirical method upon a series of Ψ scans for **2**. Unit cell parameters were obtained by a least-squares refinement of the angular settings of 25 high angle reflections ($25° < 2\theta < 30°$). Positions of ruthenium atoms were determined from the Patterson map and all other non-hydrogen atoms were subsequently located by an alternative series of Fourier synthesis and block-diagonal least-squares refinement. Finally, the structure was refined with anisotropic temperature factors. The structure refinements converged smoothly for both **1** and **2**. Hydrogen atoms were not included in the calculations. All the calculations were performed with the Universal Crystallographic Computer Program System UNICS III[21] on an ACOS-2000 computer at the Computer Center of Tohoku University. Crystallographic data, atomic coordinates and equivalent thermal parameters, and selected bond distances and angles are summarized in Tables 1—4.

Measurements. Electronic absorption spectra were recorded on a Hitachi 330 spectrophotometer. ^{1}H and ^{13}C NMR spectra were obtained on a JEOL GSX-270 FT NMR spectrometer at 270 and 67.9 MHz, respectively. Infrared absorption spectra were recorded with KBr pellets on a Jasco IR-810 spectrophotometer. Electrochemical measurements were carried out by using a Yanaco P-1100 polarographic analyzer and by use of glassy carbon (working), platinum wire (counter), and Ag/Ag$^+$ ([AgClO$_4$]=0.1 M, 1 M=1 mol dm^{-3}) (reference) electrode. Mass spectra were

Table 1. Crystallographic Data for $[Ru_3(\mu_3\text{-}O)(\mu\text{-}C_6H_5COO)_6(py)_3](PF_6)$ (**1**) and $[Ru_2(\mu\text{-}C_6H_5COO)_4Cl]$ (**2**)

Compound	**1**	**2**
Formula	$C_{57}F_6H_{45}N_3O_{13}PRu_3$	$C_{28}ClH_{20}O_8Ru_2$
Fw	1428.23	722.07
Crystal system	Hexagonal	Monoclinic
Space group	$P6_3$	$C2/c$
a/Å	13.619(6)	21.668(10)
b/Å	13.619(6)	10.741(8)
c/Å	19.204(9)	12.797(5)
β/deg		110.22(4)
V/Å^3	3085(3)	2795(3)
Z	2	4
d_{calcd}/g cm^{-3}	1.54	1.72
d_{obsd}/g cm^{-3} $^{a)}$	1.58	1.73
μ/cm^{-1}	8.2	12.0
Cryst size/mm	0.25×0.25×0.26	0.05×0.10×0.15
T/K	286	286
Radiation	Mo *Kα* (λ=0.71069 Å)	Mo *Kα* (λ=0.71069 Å)
2θ/deg	$3 \leq 2\theta \leq 70$	$3 \leq 2\theta \leq 55$
No. of unique data	2903	2997
$R^{b)}$	0.0621	0.0563
$R_w$$^{c)}$	0.0653	0.0535

a) Measured with $CHBr_3/CHCl_3$. b) $R=\sum||F_o|-|F_c||/\sum|F_o|$.
c) $R_w=[\sum w(|F_o|-|F_c|)^2/\sum w|F_o|^2]^{1/2}$, where $w=1/\sigma(|F_o|)^2$.

Table 2. Atomic Coordinates (×10^4) and Equivalent Temperature Factors for $[Ru_3(\mu_3\text{-}O)(\mu\text{-}C_6H_5COO)_6(py)_3](PF_6)$ (**1**)

Atom	x	y	z	$B_{eq}$$^{a)}$/Å^2	Atom	x	y	z	$B_{eq}$$^{a)}$/Å^2
Ru	5099(1)	2965(1)	2500(1)	2.2	C6	4589(13)	5980(12)	355(8)	4.6
P	0	0	5007(10)	3.1	C7	4757(11)	5385(14)	941(9)	5.0
O1	6667	3333	2467(18)	3.1	C8	6144(9)	5002(9)	3429(5)	2.8
F1	1097(6)	441(6)	4498(4)	4.1	C9	5896(9)	5668(8)	3975(5)	2.7
F2	−1103(7)	−456(8)	5448(5)	5.6	C10	6797(7)	6683(8)	4248(6)	2.8
O2	5290(6)	3994(7)	1700(4)	3.3	C11	6641(12)	7367(12)	4739(8)	4.5
O3	7138(7)	5411(7)	1785(5)	4.1	C12	5489(12)	7033(13)	4924(10)	5.5
O4	5339(6)	4239(6)	3156(5)	3.4	C13	4633(10)	6121(12)	4567(8)	4.6
O5	7153(7)	5366(7)	3263(5)	4.2	C14	4838(9)	5403(9)	4152(7)	3.5
N	3370(6)	2559(6)	2545(12)	2.5	C15	2895(11)	2476(12)	1858(8)	4.5
C1	6153(8)	5041(8)	1569(5)	2.4	C16	1708(14)	2221(17)	1896(11)	6.8
C2	5953(8)	5767(9)	1094(6)	2.9	C17	1131(9)	2043(12)	2548(25)	5.4
C3	6892(12)	6673(11)	752(7)	4.2	C18	1686(10)	2138(12)	3126(7)	4.2
C4	6599(11)	7256(9)	257(7)	3.8	C19	2774(8)	2397(9)	3086(6)	3.0
C5	5531(11)	6951(10)	75(7)	3.5					

a) The equivalent isotropic thermal parameter, B_{eq}, is calculated as $(4/3)\sum_j\sum_i\beta_{ij}\boldsymbol{a}_i\cdot\boldsymbol{a}_j$.

Table 3. Atomic Coordinates (×10^4) and Equivalent Temperature Factors for [Ru$_2$(μ-C$_6$H$_5$COO)$_4$Cl] (2)

Atom	x	y	z	$B_{eq}$$^{a)}$/Å^2	Atom	x	y	z	$B_{eq}$$^{a)}$/Å^2
Ru	−18(1)	482(1)	787(1)	2.0	C5	3014(4)	−2494(10)	2984(9)	7.9
Cl	0	1683(2)	2500	3.7	C6	2751(4)	−2745(8)	1866(8)	6.4
O1	933(2)	−1108(4)	72(3)	2.9	C7	2098(4)	−1163(8)	2911(6)	5.3
O2	898(2)	−161(4)	1610(3)	2.9	C8	465(3)	2051(5)	−587(4)	2.3
O3	342(2)	2030(3)	324(3)	2.7	C9	680(3)	3229(5)	−944(4)	2.7
O4	397(2)	1084(3)	−1198(3)	2.7	C10	879(3)	3219(6)	−1867(5)	3.6
C1	1180(3)	−857(5)	1101(5)	3.0	C11	1063(4)	4361(7)	−2225(7)	5.4
C2	1831(3)	−1407(6)	1763(6)	3.7	C12	1009(4)	5474(7)	−1696(7)	5.6
C3	2138(4)	−2206(7)	1209(7)	5.3	C13	810(4)	5455(7)	−757(7)	5.2
C4	2702(4)	−1724(9)	3529(7)	6.8	C14	651(3)	4315(5)	−376(6)	3.6

a) The equivalent isotropic thermal parameter, B_{eq}, is calculated as $(4/3)\sum_j\sum_i \beta_{ij} \boldsymbol{a}_i \cdot \boldsymbol{a}_j$.

Table 4. Selected Bond Distances (Å) and Angles (deg) for [Ru$_3$(μ_3-O)(μ-C$_6$H$_5$COO)$_6$(py)$_3$](PF$_6$) (1) and [Ru$_2$(μ-C$_6$H$_5$COO)$_4$Cl] (2)

Compoud **1**							
Ru···Ru′	3.350(2)	C8–C9	1.530(18)	O1–Ru′–O5	95.6(8)	O2–Ru–N	87.3(6)
Ru–O1	1.935(2)	N–C15	1.448(26)	Ru–O2–C1	128.6(7)	O3–Ru′–N	86.4(5)
Ru–N	2.134(8)	C15–C16	1.476(25)	Ru′–O3–C1	134.9(7)	O4–Ru–N	83.2(5)
Ru–O2	2.007(9)	C16–C17	1.432(48)	O2–C1–O3	124.2(11)	O5–Ru′–N	84.2(6)
Ru′–O3	2.009(11)	C17–C18	1.313(44)	O2–C1–C2	118.3(9)	Ru–N–C15	112.0(12)
Ru–O4	2.034(9)	C18–C19	1.343(19)	O3–C1–C2	117.4(8)	N–C15–C16	111.5(14)
Ru′–O5	2.026(12)	N–C19	1.268(22)	Ru–O4–C8	134.7(10)	C15–C16–C17	121.8(19)
C1–O2	1.343(10)			Ru′–O5–C8	131.8(7)	C16–C17–C18	118.9(14)
C1–O3	1.245(14)	Ru–O1–Ru	119.9(1)	O4–C8–O5	125.8(12)	C17–C18–C19	118.8(17)
C1–C2	1.468(17)	O1–Ru–O2	93.0(8)	O4–C8–O9	116.1(11)	C18–C19–N	128.3(12)
C8–O4	1.191(11)	O1–Ru–O4	96.5(7)	O5–C8–C9	117.8(9)	C19–N–C15	120.7(10)
C8–O5	1.247(15)	O1–Ru′–O3	94.0(8)	O1–Ru–N	179.6(12)	C19–N–Ru	127.3(13)
Compound **2**							
Ru–Ru′	2.290(1)	C8–O3	1.283(7)	Ru–Ru′–O4	89.6(1)	O2–C1–C2	117.8(5)
Ru–Cl	2.532(1)	C8–O4	1.277(7)	Cl–Ru–O1	91.1(1)	O1–Ru–O3	88.4(2)
Ru–O1	2.021(4)	C8–C9	1.474(8)	Cl′–Ru′–O2	90.3(1)	O2–Ru′–O4	89.7(2)
Ru′–O2	2.021(4)			Cl–Ru–O3	86.7(1)	Ru–O3–C8	120.4(3)
Ru–O3	2.011(4)	Ru′–Ru–Cl	175.5(1)	Cl′–Ru′–O4	94.9(1)	Ru′–O4–C8	119.3(4)
Ru′–O4	2.021(4)	Ru–Cl–Ru′	118.8(1)	Ru–O1–C1	118.5(4)	O3–C8–O4	121.7(5)
C1–O1	1.267(7)	Ru′–Ru–O1	89.8(1)	Ru′–O2–C1	119.4(3)	O3–C8–C9	118.9(5)
C1–O2	1.278(8)	Ru–Ru′–O2	88.7(1)	O1–C1–O2	123.3(5)	O4–C8–C9	119.3(5)
C1–C2	1.492(8)	Ru′–Ru–O3	88.9(1)	O1–C1–C2	118.9(6)		

measured with a JEOL JMS-HX 110 mass spectrometer.

Results and Discussion

1. Synthetic Procedure. As described in Experimental Section, the dimeric complex, [Ru$_2$(μ-C$_6$H$_5$COO)$_4$Cl] (**2**), was isolated from the reaction mixture similarly treated as the preparation of [Ru$_3$(μ_3-O)(μ-C$_6$H$_5$COO)$_6$(py)$_3$]$^+$. This indicates a close correlation in the formation process of these two complexes. The present procedure is regarded as that for the preparation of the trinuclear complexes according to the reported preparative methods.[3] In view of the fact that present synthetic procedure with carboxylic acids other than benzoic acid does not yield generally this type of ruthenium dimer, isolation of **2** by the present method appear to be rather accidental. Presumably, it is related to the highly insoluble nature of the benzoate-bridged dimer **2** in ethanol (vide infra).

Previously, we proposed that the different dimeric complex with the unit, Ru$_2$(μ-O)(μ-CH$_3$COO)$_2$, may be the precursor to the well-known dinuclear Ru$_2$(μ-CH$_3$COO)$_4$X and trinuclear [Ru$_3$(μ_3-O)(μ-CH$_3$COO)$_6$(L)$_3$]$^+$ (L=unidentate ligand such as H$_2$O and pyridine).[22] In the present case, we also observed the formation of the Ru$_2$(μ-O)(μ-C$_6$H$_5$COO)$_2$ unit as judged from the visible absorption spectrum,[22] when aqueous ethanol (1 : 1 (v/v)) in place of neat ethanol was used as solvent.

2. Description of the Structure of [Ru$_3$(μ_3-O)(μ-C$_6$H$_5$COO)$_6$(py)$_3$](PF$_6$) (1). This compound crystallizes in hexagonal, space group $P6_3$, which is often found in crystals of carboxylate-bridged trinuclear complexes.[1] Crystal of **1** consists of [Ru$_3$(μ_3-O)(μ-C$_6$H$_5$COO)$_6$(py)$_3$]$^+$ and PF$_6^-$. An ORTEP view of the complex ion is shown in Fig. 1a along with the atomic

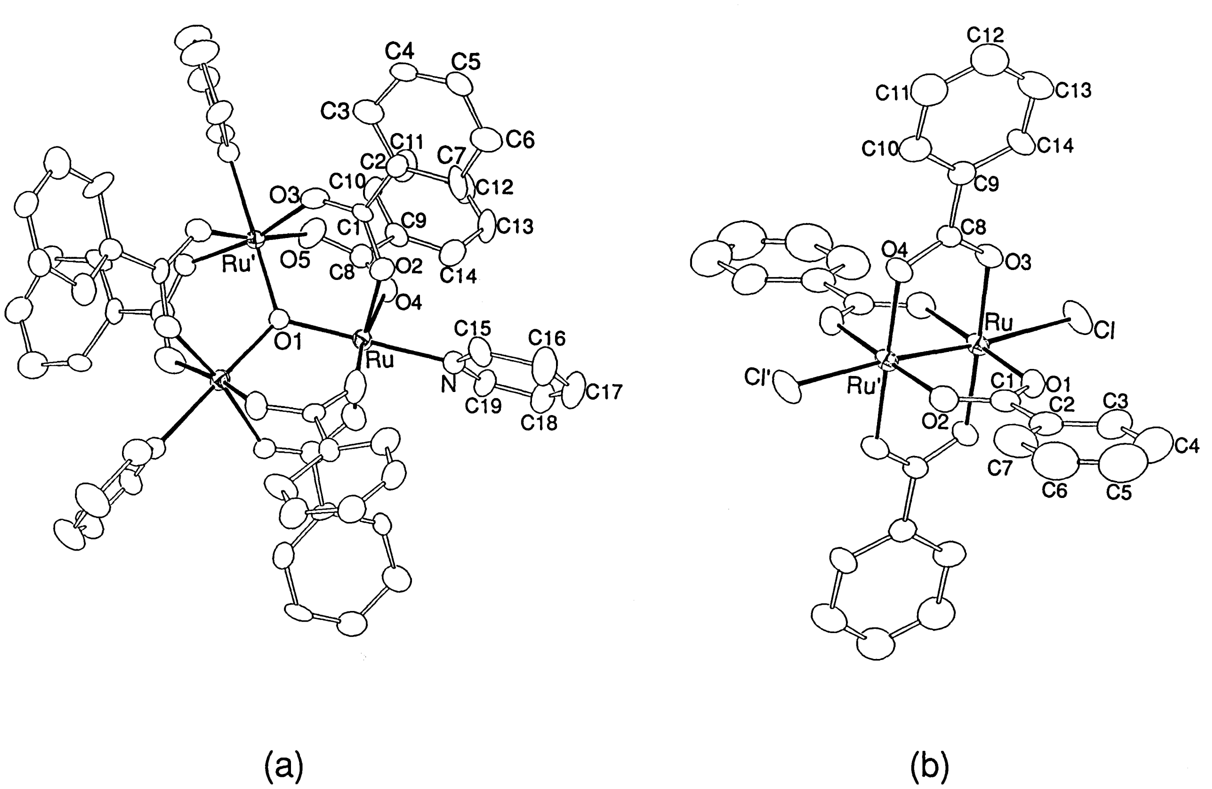

Fig. 1. (a) An ORTEP view of [Ru$_3$(μ_3-O)(μ_3-C$_6$H$_5$COO)$_6$(py)$_3$]$^+$. (b) Ru$_2$(μ-C$_6$H$_5$COO)$_4$ unit and its axial Cl atoms as they occur in [Ru$_2$(μ-C$_6$H$_5$COO)$_4$Cl] (**2**). Crystallographically independent atoms are labelled.

numbering scheme. An asymmetric unit of the cell contains one thirds of the complex ion. Three Ru^{III} ions form an equilateral triangle with a crystallographic C$_3$ axis passing through the μ_3-O atom (O1). Ru^{III} centers are in pseudooctahedral geometry, and are displaced slightly toward μ_3-O (N-Ru-O(benzoate)= 83.2(5)—87.3(6)°). Ru···Ru distance is 3.350(2) Å which is slightly longer (ca. 0.02 Å) than that in Cotton's mixed-valent (II,III,III) complex, [Ru$_3$(μ_3-O)(μ-CH$_3$COO)$_6$(PPh$_3$)$_3$].[9] This comes from the difference in Ru-(μ_3-O) distances in these two complexes (1.935(2) Å in **1** and 1.92(2) Å in the triphenylphosphine complex). The difference in the Ru-(μ_3-O) distance is opposite to the one expected from the oxidation state and is due to the kind of coordinated atom at the terminal positions (N or P). For the similar trirhodium complex, [Rh$_3$(μ_3-O)(μ-CH$_3$COO)$_6$(H$_2$O)$_3$](ClO$_4$)·nH$_2$O (n=1,2), Rh···Rh and Rh-(μ_3-O) distance are reported to be 3.32—3.35 Å and 1.90—1.94 Å, respectively.[23] Benzoate anions in **1** take usual chelating mode. Pyridine rings at the terminal positions are almost perpendicular to the "Ru$_3$(μ_3-O)" plane as has been found in [Mn$_3$(μ_3-O)(μ-C$_6$H$_5$COO)$_6$(py)$_2$(H$_2$O)]·0.5CH$_3$CN.[24] On the other hand, coordinated pyridines in acetate-bridged trinuclear complexes, [V$_3$(μ_3-O)(μ-CH$_3$COO)$_6$-(py)$_3$],[25] [Mn$_3$(μ_3-O)(μ-CH$_3$COO)$_6$(py)$_3$],[26] and [Fe$_3$(μ_3-O)(μ-CH$_3$COO)$_6$(py)$_3$](py),[27] are not perpendicular but rather coplanar to the "M$_3$(μ_3-O)" plane in the solid state.[28]

3. Other Properties of [Ru$_3$(μ_3-O)(μ-C$_6$H$_5$COO)$_6$-(py)$_3$](PF$_6$) (1).

Absorption spectrum of **1** in CH$_3$CN shows a broad peak at 705 nm (ε_{max}=6060 M^{-1} cm^{-1}), which is shifted to the longer wave-length as compared with that of the acetate-bridged analogue, [Ru$_3$(μ_3-O)(μ-CH$_3$COO)$_6$(py)$_3$](PF$_6$) (λ_{max}=690 nm, ε_{max}=5600 M^{-1} cm^{-1}) (M=mol dm^{-3}). Analogous spectral features are observed in other pyridine derivatives coordinated triruthenium complexes with the (III,III,III) oxidation state,[3,4,6,7] and the absorptions are attributed to transitions between MO levels formed by dπ(Ru)-pπ(μ_3-O) interactions.[4—7,9]

Cyclic voltammogram of **1** in 0.1 M (n-C$_4$H$_9$)$_4$NPF$_6$-CH$_3$CN at 20 °C shows four reversible one-electron processes. $E_{1/2}$ values[29] are at +1.58, +0.71, −0.26, and −1.54 V vs. Ag/Ag$^+$ (at a scan rate of 50 mV s^{-1}), which are assigned to redox couples, (+3/+2), (+2/+1), (+1/0), and (0/−1), respectively, where number in parenthesis denotes electric charge on the complex ion. Corresponding $E_{1/2}$ values of [Ru$_3$(μ_3-O)(μ-CH$_3$-COO)$_6$(py)$_3$]$^+$ are at +1.60, +0.63, −0.42 and −1.70 V under the same conditions. On going from the acetate complex to benzoate complex **1**, corresponding $E_{1/2}$'s are shifted toward positive side and differences between corresponding $E_{1/2}$'s decrease as the oxidation states increase. The redox potential for the (+3/+2) couple at the most positive side is almost identical for **1** and the acetate complex. It has been shown that there is a linear correlation between each $E_{1/2}$ value of carboxylate-bridged complex and pK_a of its free carboxylic acid for $[L_2Ru_2(\mu\text{-O})(\mu\text{-RCOO})_2]^{2+}$ (L = 1,4,7-trimethyl-1,4,7-triazacyclononane),[30] and $[Fe_3(\mu_3\text{-O})(\mu\text{-RCOO})_6(H_2O)_3]^{n+}$ (n = 1,7).[31] Toma et al. reported a similar linear relationship between $E_{1/2}$ and pK_a values of the *terminal* ligands for $[Ru_3(\mu_3\text{-O})(\mu\text{-CH}_3COO)_6(\text{N-Het})_3]$ (N-Het = pyridine and pyrazine derivatives), and they also showed that the variation of the redox potentials is relatively small at the high oxidation states, but increases as the oxidation states decrease.[6] These reported trends are consistent with the present observation for **1** and the acetate complex. The pK_a values for acetic and benzoic acid are 4.56 and 4.20, respectively.[32] Electron density in the "$Ru_3(\mu_3\text{-O})$" core is smaller for **1**, which has less basic bridging carboxylate anions.

Substitution lability at the terminal position of **1** was investigated by use of the pyridine–pyridine-d_5 exchange reaction (Eq. 1).

$$[Ru_3(\mu_3\text{-O})(\mu\text{-C}_6H_5COO)_6(py)_3]^+ + 3py\text{-}d_5 \longrightarrow [Ru_3(\mu_3\text{-O})(\mu\text{-C}_6H_5COO)_6(py\text{-}d_5)_3]^+ + 3py \qquad (1)$$

The reaction was monitored with a CD_3CN solution ([**1**]=4.7 mM) containing a large excess of py-d_5 ([py-d_5] = 387 mM) at 60 °C by means of ^{1}H NMR spectroscopy.[33] Experimental details are the same as those used in previous works on similar systems.[22,34,35] Observed first-order rate constant (k) for the substitution reaction (Eq. 1) was $4.9\times10^{-6}\,s^{-1}$ at 60 °C, which is one order of magnitude smaller than the corresponded value (k') for the acetate-bridged complex, $[Ru_3(\mu_3\text{-O})(\mu\text{-CH}_3COO)_6(py)_3](PF_6)$ ($k' = 5.0\times10^{-5}\,s^{-1}$ (60 °C)[36]). This may be ascribed to difference in pK_a of the bridging carboxylate ligand.

When compound **1** is reduced by hydrazine monohydrate in CH_3CN under N_2 atmosphere at room temperature, the color of the solution turns yellow from dark blue. The yellow color is due to the mixed-valent (II,III,III) complex, $[Ru_3(\mu_3\text{-O})(\mu\text{-C}_6H_5COO)_6(py)_3]$. Subsequent CO bubbling to this solution at 80 °C for 2 h yielded dark blue precipitates, which were identified as $[Ru_3(\mu_3\text{-O})(\mu\text{-C}_6H_5COO)_6(py)_2(CO)]$ by means of IR, ^{1}H NMR, and absorption spectra.[37] The analogous (II,III,III) complex with the same composition, $[Ru_3(\mu_3\text{-O})(\mu\text{-CH}_3COO)_6(py)_2(CO)]$, has been prepared in a similar way from $[Ru_3(\mu_3\text{-O})(\mu\text{-CH}_3COO)_6(py)_3]^+$.[4]

4. Structural Description of $[Ru_2(\mu\text{-C}_6H_5COO)_4Cl]$ (2). Figure 1b shows X-ray structure of **2** with the atomic labelling scheme. An asymmetric unit of the cell contains half of this centro-symmetric molecule. Therefore, two ruthenium ions within a molecule are crystallographically equivalent, and have the averaged oxidation state of +2.5. As shown in Fig. 2, an axial chloro ligand bridges the neighboring dimer unit at its vacant axial site, forming infinite zig-zag chains along c-axis (angles of Ru-Ru-Cl and Ru-Cl-Ru are 175.5(1)° and 118.8(1)°, respectively). Similar ···X-Ru-Ru-X-Ru-Ru-X··· chains are reported to be linear in $[Ru_2(\mu\text{-CH}_3COO)_4Cl]\cdot 2H_2O$,[12] $[Ru_2(\mu\text{-C}_2H_5COO)_4Cl]$,[12] $[Ru_2(\mu\text{-CH}_3COO)_4Cl]$,[13,38] and to be zig-zag shaped in $[Ru_2(\mu\text{-HCOO})_4Br]$,[14] $[Ru_2(\mu\text{-CH}_3COO)_4Cl]$,[15,38] $[Ru_2(\mu\text{-}(n\text{-C}_3H_7)COO)_4Cl]$,[16] $[Ru_2(\mu\text{-C}_6H_4(p\text{-OMe})COO)_4Cl]\cdot(H_2O)_{0.25}$.[17] The Ru–Ru distance in **2** is 2.290(1) Å, showing the presence of the Ru–Ru direct bond as in the analogues.

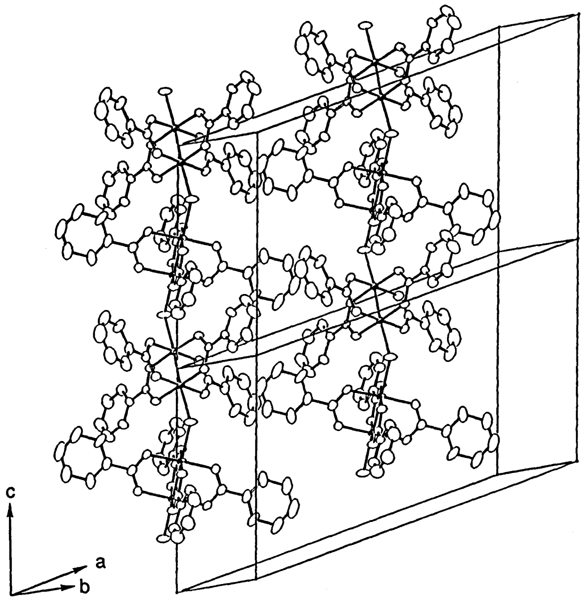

Fig. 2. Packing Diagram of $[Ru_2(\mu\text{-C}_6H_5COO)_4Cl]$ (**2**). Two unit cells are shown.

Compound **2** is very slightly soluble in DMF and DMSO, but practically insoluble in other common organic solvents and water. A DMF solution of **2** shows absorption maxima at 580 (shoulder), 456 and 303 nm. Solid state diffuse reflectance spectrum of **2** shows absorption maxima at 520 and 470 nm. The spectral differnce appears to reflect structural difference between solution and solid state. Similar phenomenon was observed for $[Ru_2(\mu\text{-CH}_3COO)_4Cl]$.[39]

Tables of anisotropic thermal parameters, all the bond distances and angles, and observed and calculated structure factors for **1** and **2** are deposited as Document No. 9002 at the Office of the Editor of Bull. Chem. Soc. Jpn.

This work was supported by a Grant-in-Aid for Scientific Research (No. 01430009) and a Grant-in-Aid for Scientific Research No. 02245106 on Priority Area of "Molecular Approaches to Non-equilibrium Processes in Solutions" from the Ministry of Education, Science, and Culture.

References

1) R. D. Cannon and R. P. White, *Prog. Inorg. Chem.*, **36**, 195 (1988).

2) For example: $[Ru_3(\mu_3\text{-O})(\mu\text{-CH}_3COO)_6(L)_3]^{n+}$ {n=0: $(L)_3 = (PPh_3)_3$,[3,9] $(py)_2(CO)$,[4]; n = 1: $(L)_3 = (H_2O)_3$,[3,5] $(MeOH)_3$,[4]

$(py)_2(MeOH)$,[4] (pyridine derivatives)$_3$;[6,7] $n=0$—2: $(L)_3=(py)_3$,[4] $(py)_2(pyr)$,[4]}, $[Ru_3(\mu_3\text{-}O)(\mu\text{-}RCOO)_6(L)_3]^+$ ($R=C_2H_5$, $n\text{-}C_3H_7$; $L=H_2O$, py, PPh_3),[3] and $[Ru_3(\mu_3\text{-}O)(\mu\text{-}C_6H_5COO)_6(H_2O)_3]$,[3] where pyr = pyrazine.

3) A. Spencer and G. Wilkinson, *J. Chem. Soc., Dalton Trans.*, **1972**, 1570.

4) J. A. Baumann, D. J. Salmon, S. T. Wilson, and T. J. Meyer, *Inorg. Chem.*, **17**, 3342 (1978).

5) Y. Sasaki, A. Tokiwa, and T. Ito, *J. Am. Chem. Soc.*, **109**, 6341 (1987).

6) H. E. Toma, C. J. Cunha, and C. Cipriano, *Inorg. Chim. Acta*, **154**, 63 (1988).

7) H. E. Toma and C. J. Cunha, *Can. J. Chem.*, **67**, 1632 (1989).

8) H. Kobayashi, N. Uryu, A. Tokiwa, T. Yamaguchi, Y. Sasaki, and T. Ito, *Bull. Chem. Soc. Jpn.*, **65**, 198 (1992).

9) F. A. Cotton and J. G. Norman, Jr., *Inorg. Chim. Acta*, **6**, 411 (1972).

10) For example: $[Ru_2(\mu\text{-}HCOO)_4X]$ (X = Cl, Br, I),[14] $[Ru_2(\mu\text{-}CH_3COO)_4X]$ (X = Cl,[12–15] Br,[14]), $[Ru_2(\mu\text{-}C_2H_5COO)_4Cl]$,[12] $[Ru_2(\mu\text{-}(n\text{-}C_3H_7)COO)_4Cl]$,[16] $[Ru_2(\mu\text{-}C_6H_5COO)_4X]$ (X = Cl,[11,14] Br[11]), and $[Ru_2(\mu\text{-}C_6H_4(p\text{-}OMe)COO)_4Cl](H_2O)_{0.25}$.[17]

11) B. K. Das and A. R. Chakravarty, *Polyhedron*, **7**, 685 (1988).

12) A. Bino, F. A. Cotton, and T. R. Felthouse, *Inorg. Chem.*, **18**, 2599 (1979).

13) D. S. Martin, R. A. Newman, and L. M. Vlasnic, *Inorg. Chem.*, **19**, 3404 (1980).

14) M. Mukaida, T. Nomura, and T. Ishiomori, *Bull. Chem. Soc. Jpn.*, **45**, 2143 (1972).

15) T. Togano, M. Mukaida, and T. Nomura, *Bull. Chem. Soc. Jpn.*, **53**, 2085 (1980).

16) M. J. Bennett, K. G. Caulton, and F. A. Cotton, *Inorg. Chem.*, **8**, 1 (1969).

17) B. K. Das and A. R. Chakravarty, *Polyhedron*, **10**, 491 (1991).

18) Electronic absorption spectrum of this reaction mixture resembled that of $[Ru_3(\mu_3\text{-}O)(\mu\text{-}CH_3COO)_6(H_2O)_3]^+$.

19) This compound is paramagnetic, although it shows relatively sharp ^1H NMR signals. Signal assignments were made on the basis of relative integrated intensity ratio and signal assignments for similarly paramagnetic $[Ru_3(\mu_3\text{-}O)(\mu\text{-}CH_3COO)_6(py)_3](PF_6)$.[4]

20) M denotes $[Ru_3(\mu_3\text{-}O)(\mu\text{-}C_6H_5COO)_6(py)_3]^+$.

21) T. Sakurai and K. Kobayashi, *Rikagaku Kenkyusho Houkoku*, **55**, 69 (1979).

22) Y. Sasaki, M. Suzuki, A. Nagasawa, A. Tokiwa, M. Ebihara, T. Yamaguchi, C. Kabuto, T. Ochi, and T. Ito, *Inorg. Chem.*, **30**, 4903 (1991).

23) T. Glowiak, M. Kubiak, and T. Szymanska-Buzar, *Acta Crystallogr., Sect. B*, **33**, 1732 (1977).

24) J. B. Vincent, H.-R. Chang, K. Folting, J. C. Huffman, G. Christou, and D. N. Hendrickson, *J. Am. Chem. Soc.*, **109**, 5703 (1987).

25) F. A. Cotton, M. W. Extine, L. R. Falvello, D. B. Lewis, G. E. Lewis, C. A. Murillo, W. Schwotzer, M. Tomas, and J. M. Troup, *Inorg. Chem.*, **25**, 3505 (1986).

26) A. R. E. Baikie, M. B. Hursthouse, D. B. New, and P. Thornton, *J. Chem. Soc., Chem. Commun.*, **1978**, 62.

27) S. E. Woehler, R. J. Wittebort, S. M. Oh, T. Kambara, D. N. Hendrickson, D. Inniss, and C. E. Strouse, *J. Am. Chem. Soc.*, **109**, 1063 (1987).

28) Very recently, crystal structure of $[Ga_3(\mu_3\text{-}O)(\mu\text{-}C_6H_5COO)_6(4\text{-}Mepy)_3]GaCl_4\cdot 4\text{-}Mepy$ (4-Mepy = 4-methylpyridine) was reported, in which two 4-Mepy rings are approximately parallel and the third one is perpendicular to the "$Ga_3(\mu_3\text{-}O)$" plane: M. T. Andras, S. A. Duraj, A. F. Hepp, P. E. Fanwick, and M. M. Bodnar, *J. Am. Chem. Soc.*, **114**, 786 (1992).

29) $E_{1/2}=(E_{pa}+E_{pc})/2$.

30) P. Neubold, K. Wieghardt, B. Nuber, and J. Weiss, *Inorg. Chem.*, **28**, 459 (1989).

31) K. Nakata, A. Nagasawa, Y. Sasaki, and T. Ito, *Chem. Lett.*, **1989**, 753.

32) A. E. Martell and R. M. Smith, "Critical Stability Constants," Plenum, London and New York (1977).

33) Decrease in integrated intensity of the signal due to 3,5-H of coordinated pyridine and increase in that of 2,6-H of free pyridine were followed.

34) M. Abe, Y. Sasaki, A. Nagasawa, and T. Ito, *Bull. Chem. Soc. Jpn.*, **65**, 1411 (1992).

35) K. Nakata, A. Nagasawa, N. Soyama, Y. Sasaki, and T. Ito, *Inorg. Chem.*, **30**, 1575 (1991).

36) Rate constant k' was evaluated from activation parameters of $\Delta H^{\neq}$ (=123 kJ mol^{-1}) and $\Delta S^{\neq}$ (=41 J K^{-1} mol^{-1}) in Ref. 34.

37) IR (KBr) 1940 cm^{-1} (ν (CO)); UV-vis (CH_2Cl_2) λ_{max} =600, 305, 270 nm; ^1H NMR (CD_2Cl_2) δ=7.25 (12H, Ph-3,5-H), 7.51 (6H, Ph-4-H), 7.68 (12H, Ph-2,6-H), 8.28 (2H, py-3,5-H), 8.30 (4H, py-4-H), 9.44 (4H, py-2,6-H). ^1H NMR spectrum showed the presence of a small amount of starting material, $[Ru_3(\mu_3\text{-}O)(\mu\text{-}C_6H_5COO)_6(py)_3]^+$.

38) There are two crystal modifications in this compound.

39) Absorption spectrum in CH_3CN: λ_{max}=1000 nm (ε_{max}=27 M^{-1} cm^{-1}) and 427 (755); Diffuse reflectance spectrum (MgO pellet): λ_{max}=510, 465 nm.